

Electronic Supplementary Information

Exciton energy transfer and bi-exciton annihilation in the emitting layers of thermally activated delayed fluorescence-based OLEDs

Hyunchul Kang,¹ Han Jin Ahn,² Gyeong Woo Kim,² Ji-Eun Jeong,¹ Han Young Woo,¹ Jun-Yun Kim,^{2,} and Sungnam Park^{1,*}*

¹Department of Chemistry and Research Institute for Natural Science, Korea University, 145 Anam-ro, Seongbuk-gu, Seoul, 02841, Republic of Korea

²LG Display Co. Ltd., LG Science Park, 30, Magokjungang 10-ro, Gangseo-gu, Seoul, 07796, Republic of Korea

Corresponding Authors:

*E-mail: windwart@lgdisplay.com (J. Y. Kim) and spark8@korea.ac.kr (S. Park)

1. TADF kinetic model with the concentration quenching of triplet excitons

Time-resolved PL (TRPL) spectra of DPEPO:TDBA-DI films were analyzed by a conventional TADF kinetic model with a concentration quenching of triplet excitons. The coupled differential equations for the concentrations of singlet and triplet excitons ($[S_1]$ and $[T_1]$) can be written by,

$$\frac{d[S_1](t)}{dt} = -(k_r^S + k_{nr}^S + k_{ISC})[S_1](t) + k_{RISC}[T_1](t) \quad (s1)$$

$$\frac{d[T_1](t)}{dt} = k_{ISC}[S_1](t) - (k_{nr}^T + k_{RISC})[T_1](t) - k_{TTA}[T_1]^2(t) \quad (s2)$$

where k_r^S is the radiative rate constant of the excited singlet state, k_{nr}^S is the non-radiative rate constant of the excited singlet state, k_{ISC} is the intersystem crossing rate constant from the excited singlet state to the excited triplet state, k_{RISC} is the reverse intersystem crossing rate constant from the excited triplet state to the excited singlet state, k_{nr}^T is the non-radiative rate constant of the excited triplet state, and k_{TTA} is the rate constant of the concentration quenching of triplet excitons. The solution of Eqs. (s1) and (s2) is obtained by

$$[S_1](t) = A_{PF} \exp(-t/\tau_{PF}) + A_{DF} \exp(-t/\tau_{DF}) \quad (s3)$$

where $\tau_{PF} = 1/k_{PF}$ and $\tau_{DF} = 1/k_{DF}$ were obtained by fitting a multi-exponential function $I(t) = \sum_{i=1}^n A_i \exp(-t/\tau_i)$ to TRPL signals. The prompt and delayed fluorescence rate constants, k_{PF} and k_{DF} , are given by

$$k_{PF} + k_{DF} = k_r^S + k_{nr}^S + k_{ISC} + k_r^T + k_{nr}^T + k_{RISC} + k'_{TTA} \quad (s4)$$

$$k_{PF}k_{DF} = (k_r^S + k_{nr}^S + k_{ISC})(k_r^T + k_{nr}^T + k_{RISC} + k'_{TTA}) - k_{ISC}k_{RISC} \quad (s5)$$

where $k'_{TTA} = k_{TTA}[T_1]$. By assuming that $k_{PF} \gg k_{DF}$, $k_r^S \gg k_{nr}^S, k_{RISC}$, $k_{RISC} \gg k_r^T, k_{nr}^T, k'_{TTA}$, and $k_{nr}^S \approx 0, k_{nr}^T \approx 0$ because of high PLQY, the rate constants can be simply obtained as,

$$k_{PF} = 1/\tau_{PF} \approx k_r^S + k_{ISC} \quad (s6)$$

$$k_{DF} = 1/\tau_{DF} \quad (s7)$$

$$k_r^S = k_{PF} \cdot \Phi_{PF} \quad (s8)$$

$$k_{ISC} \approx k_{PF} \cdot (1 - \Phi_{PF}) \quad (s9)$$

$$k_{RISC} = (k_{DF} - k_{nr}^T) / \Phi_{PF} \approx k_{DF} / \Phi_{PF} \quad (s10)$$

On the other hand, when the concentration quenching of triplet excitons occurs and k'_{TTA} is comparable to k_{RISC} , Eqs. (s4) and (s5) are reduced to

$$k_{PF} + k_{DF} \approx k_r^S + k_{ISC} + k_{RISC} + k'_{TTA} \quad (s11)$$

$$k_{PF}k_{DF} \approx k_r^S k_{RISC} + k_r^S k'_{TTA} + k_{ISC} k'_{TTA} \quad (s12)$$

Solving Eqs. (s11) and (s12) for k'_{TTA} ,

$$k'_{TTA} = \frac{1}{2} \left(k_{PF} + k_{DF} - 2k_{RISC} - \sqrt{(k_{PF} - k_{DF})^2 - 4k_{ISC}k_{RISC}} \right) \quad (s13)$$

The rate constant for the concentration quenching of triplet states $k'_{TTA} = k_{TTA}[T_1]$ can be determined once k_{PF} , k_{DF} , k_{ISC} , and k_{RISC} are experimentally measured.

In our experiments, k_{ISC} and k_{RISC} were assumed to be concentration-independent for DPEPO:TDBA-DI films. The k_{ISC} and k_{RISC} values obtained from DPEPO:TDBA-DI film (90:10 wt%) were used to determine k'_{TTA} for DPEPO:TDBA-DI films (70:30 and 50:50 wt%).

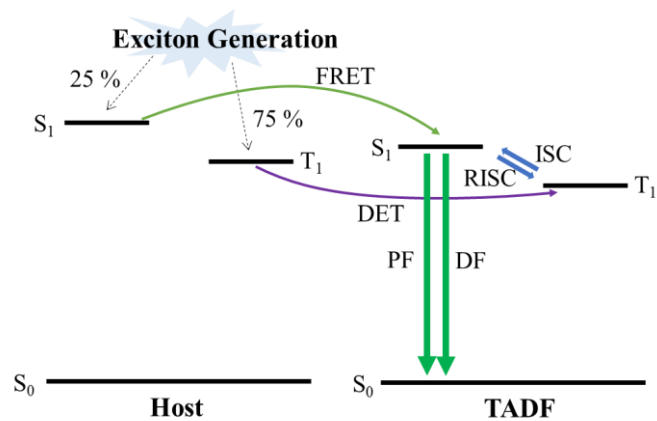


Figure S1. Electroluminescence (EL) mechanism of TADF-based OLEDs.

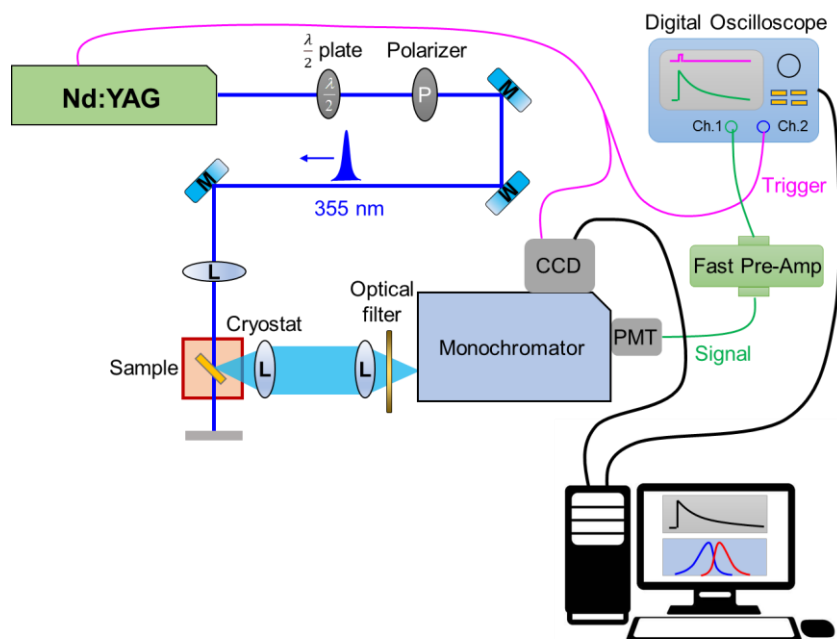


Figure S2. Schematic illustration of our TRPL experimental setup.

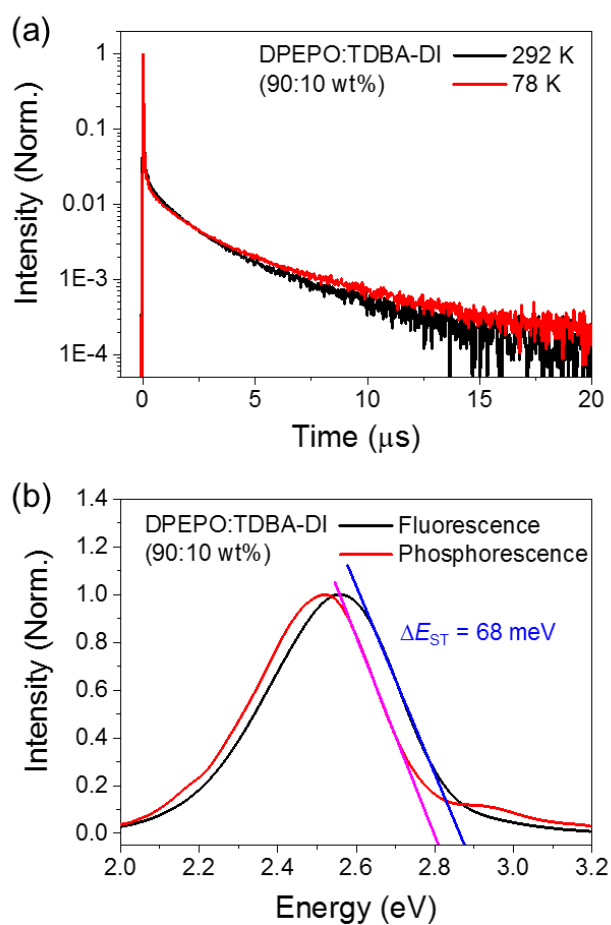


Figure S3. (a) TRPL signals of DPEPO:TDBA-DI film (90:10 wt%) measured at 292 K and 78 K. (b) Fluorescence and phosphorescence spectra of DPEPO:TDBA-DI film (90:10 wt%) measured at 78 K ($\Delta E_{\text{ST}} = 68 \text{ meV}$).

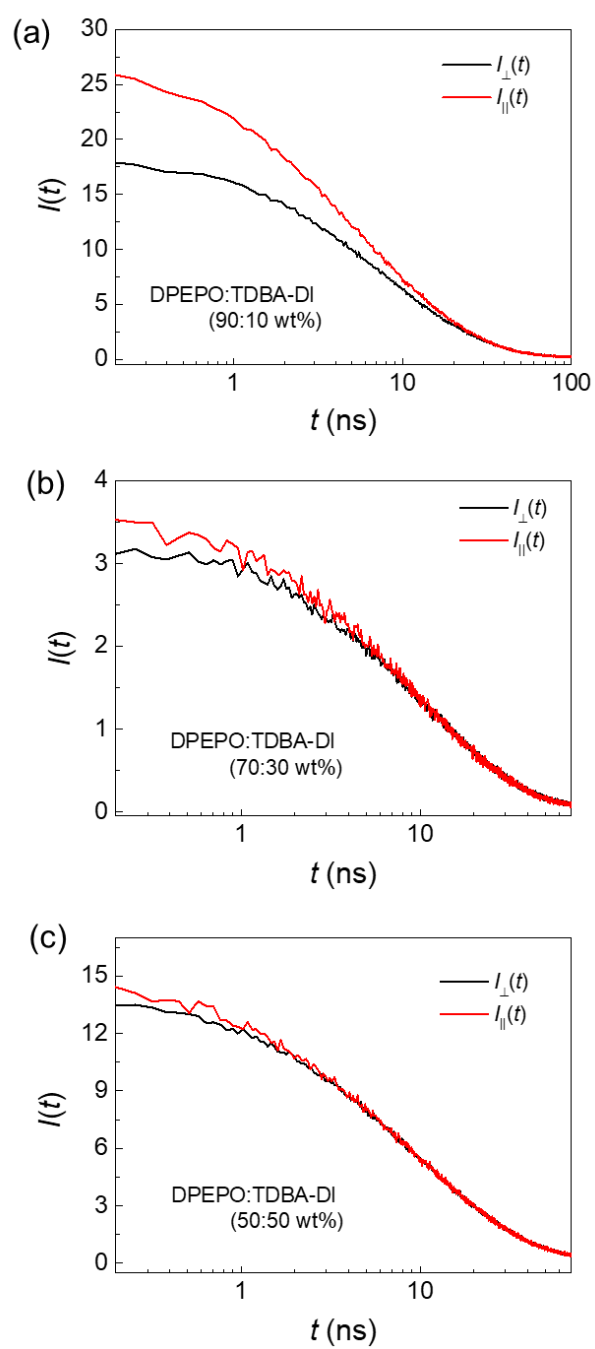


Figure S4. Intensity-calibrated $I_{\parallel}(t)$ and $I_{\perp}(t)$ measured with DPEPO:TDBA-DI films. (a) 90:10, (b) 70:30, and (c) 50:50 wt%.

Table S1. The number of host and dopant molecules (n_{host} and n_{dopant}) used for the MD simulations. The volume, V_{box} , of the simulation box for DPEPO:TDBA-DI films.

| DPEPO:TDBA-DI (wt%) | n_{host} | n_{dopant} | V_{box} (nm ³) |
|---------------------|-------------------|---------------------|-------------------------------------|
| 90 : 10 | 560 | 39 | 497.8 |
| 70 : 30 | 467 | 133 | 565.6 |
| 50 : 50 | 359 | 240 | 628.5 |

Table S2. Parameters for the fit of a Gaussian function to the distribution of the minimum distances of all pairs of TDBA-DI molecules in films: mean, $d_{\text{min,center}}$, standard deviation, w , and R^2 values.

| DPEPO:TDBA-DI (wt%) | $d_{\text{min,center}}$ (nm) | w (nm) | R^2 |
|---------------------|------------------------------|----------|-------|
| 90 : 10 | 1.30 | 0.87 | 0.51 |
| 70 : 30 | 0.85 | 0.58 | 0.87 |
| 50 : 50 | 0.72 | 0.48 | 0.95 |

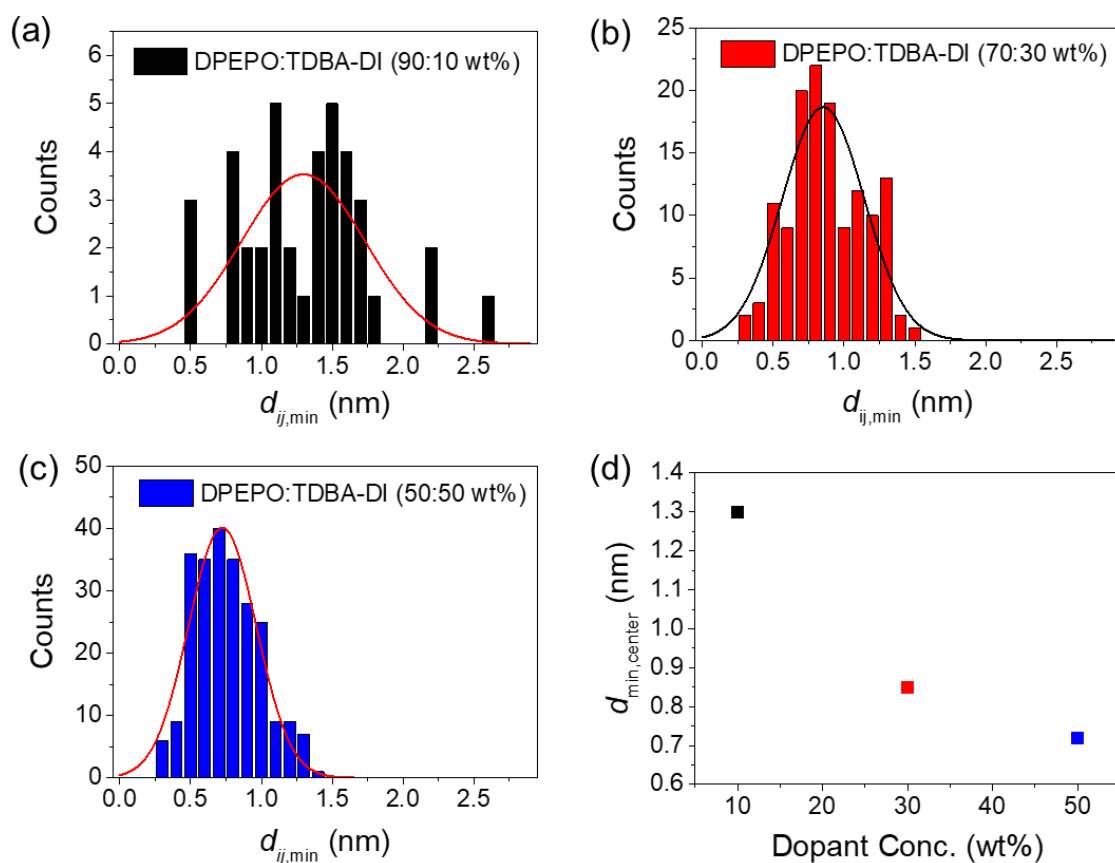


Figure S5. Distribution of the minimum distances, $d_{ij,\min}$, of all pairs of neighboring TDBA-DI molecules in films: (a) 90:10, (b) 70:30, and (c) 50:50 wt%. The distribution is fitted by a Gaussian function. (d) Comparison of the average minimum distances of neighboring TDBA-DI molecules in films.

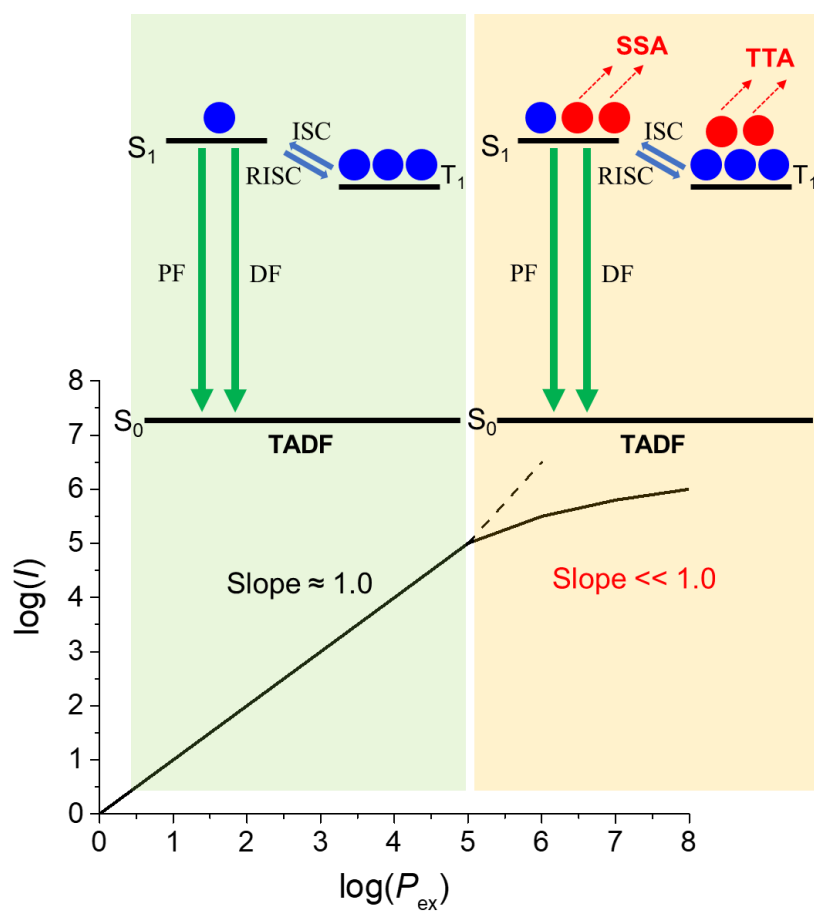


Figure S6. Exciton-exciton annihilation mechanism (bi-exciton recombination) in TADF-based OLEDs when the excitation laser power is increased.

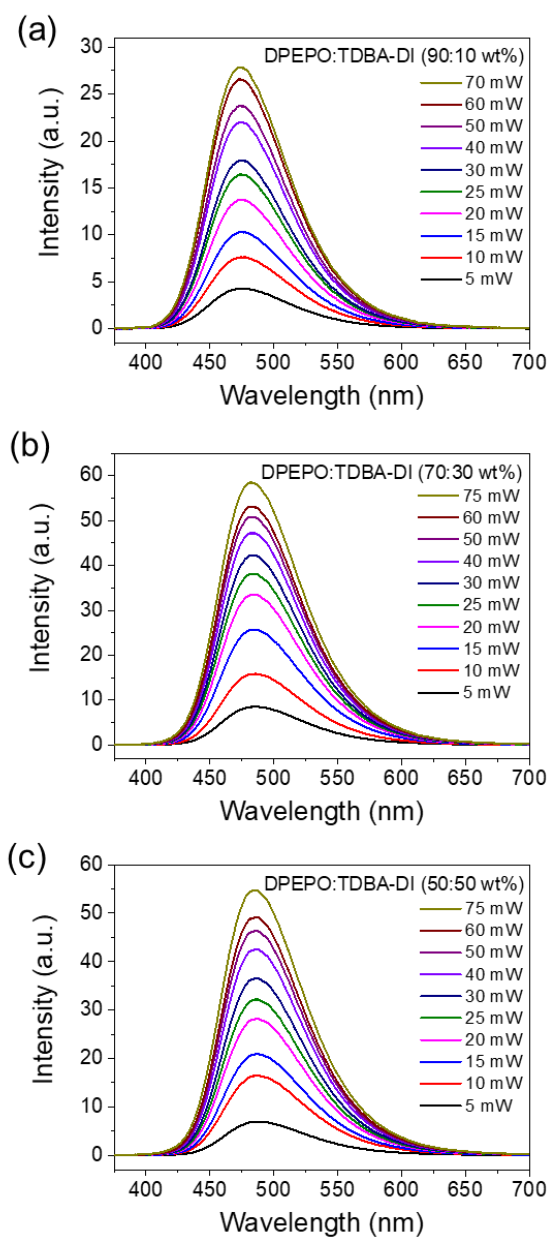


Figure S7. Excitation power-dependent PL spectra of DPEPO:TDBA-DI films. (a) 90:10, (b) 70:30, and (c) 50:50 wt%.

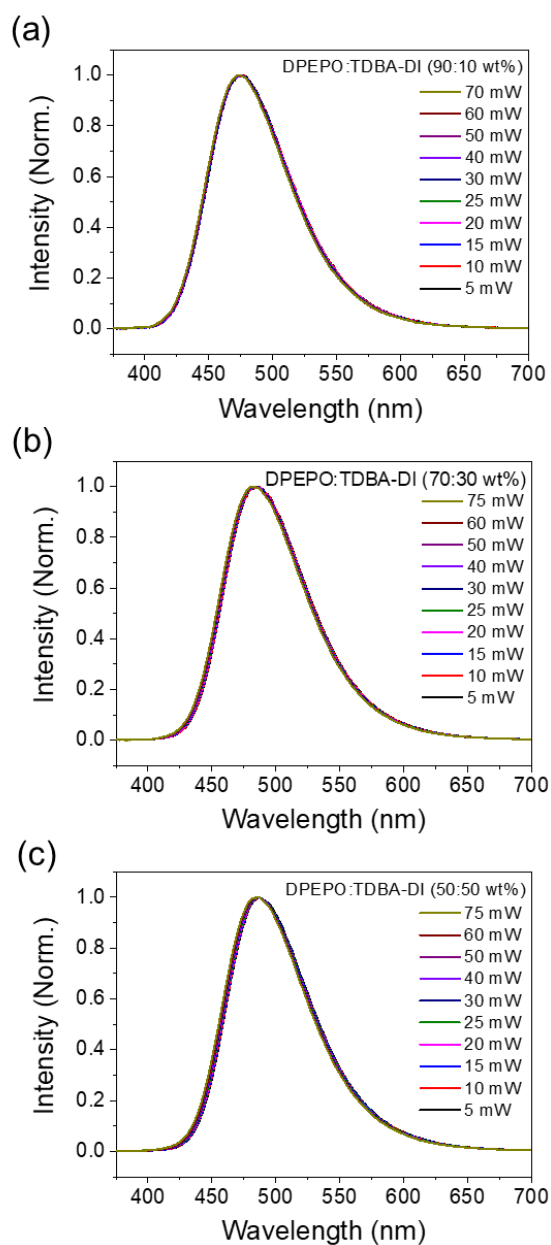


Figure S8. Normalized excitation power-dependent PL spectra of DPEPO:TDBA-DI films. (a) 90:10, (b) 70:30, and (c) 50:50 wt%.